JUNE 1981 LRP 182/81

QUASI-STEADY TURBULENCE DRIVEN BY RUNAWAY ELECTRONS

L. Muschietti, K. Appert, and J. Vaclavik

QUASI-STEADY TURBULENCE DRIVEN BY RUNAWAY ELECTRONS

L. Muschietti, K. Appert, and J. Vaclavik

Centre de Recherches en Physique des Plasmas
Association Euratom - Confédération Suisse
Ecole Polytechnique Fédérale de Lausanne
CH-1007 Lausanne, Switzerland

ABSTRACT

The evolution of the turbulence driven by runaway electrons has been followed by means of a computer code based on the quasi-linear equations. The evolution is not characterized by periodic relaxations as claimed in previous works but ends in a quasi-steady turbulent, yet very persistent state, accessible from different initial conditions. This discrepancy is clarified as being due to the excessive stiffness of the moment equations used to demonstrate the relaxations. Moreover, a theory is developed to interpret the quasi-steady state found.

I. INTRODUCTION

Five years ago, the pioneering work of Parail and Pogutse[1] indicated how runaway electrons could drive a kinetic instability in toroidal discharges via the anomalous Doppler effect. The authors attempted to provide a theory for the runaway instability observed in tokamaks[2] which exhibits relaxations with a period of a few collision times. Numerous papers published afterward were devoted mainly to the study of the development of one burst and its possible macroscopic consequences. It was tacitly admitted that, after the saturation of the instability (one burst) due to the quasi-linear change of the distribution function, the system was somehow recycled to a state from which the instability could grow up again. In fact, the periodicity, a crucial point of the observation which it was attempted to interpret theoretically, has as yet only been mathematically demonstrated in two papers[1,3]; the proof, however, is based on moment equations, the use of which to describe kinetic effects is questionable. Thus, it is highly desirable to follow the evolution by means of the quasi-linear equations themselves over a long time interval.

For this purpose we have extended our quasi-linear numerical code, based on the Ritz-Galerkin method and special finite elements,[4] to the problem of the runaway instability. It comprises the quasi-linear terms due to Cerenkov and anomalous Doppler effects as well as the terms corresponding to the electric field and the Coulomb collisions. So, the code allows us to study the dynamics of the formation and destruction of the runaway tail in a consistent manner. We do not need to introduce arguments of little conviction on the different time scales involved in order to separate the roles played by the Cerenkov and anomalous Doppler effects, on the one hand, from those of the electric field and collisions, on the other hand. In fact, the interplay between the different terms turns out to be very important since we find that, after one burst, the time-scale of the turbulence adapts itself to that of the electric field, which leads to a quasi-stationary highly non-Maxwellian but very stable state. In contrast to previous work, it is fairly simple to describe a posteriori the turbulent state attained by the system using an analytical model. In this model the Cerenkov and anomalous Doppler interactions act as convertors of the work furnished by the electric field into the energy of the Langmuir fluctuations and the gyration energy of the electrons.

The plan of the paper is as follows: In Sec. II we formulate the problem, discuss the onset of the turbulence and report on the development of the instability as found from our computations. Section III is devoted to the theory of the quasi-steady state; successively we discuss its stability and present the equations and formulae of the model. Finally, we use them for two brief applications in Sec. IV.

II. DYNAMICS

A. Formulation of the problem

Let us apply a weak electric field to a strongly magnetized, homogeneous plasma. The existence of Coulomb collisions prevents the electron distribution from shifting away in velocity space, which results in the growing of a runaway tail. This distortion of the initial Maxwellian distribution may destabilize the plasma waves with frequencies $\omega_k = \omega_{pe} k_{\parallel}/k$ that, in turn, modify the distribution function. Thus, a consistent kinetic calculation should simultaneously take into account the electric field, collisions, and collective effects. The relevant quasilinear equations, normalized according to $k \to k/\lambda_D$, $v \to v\, v_{te}$, $t \to t/\omega_{pe}$, $f \to fn/v_{te}^3$, $\varepsilon_k \to \varepsilon_k 4\pi n T \lambda_D{}^3$, are

$$\frac{\partial}{\partial t} f(v_\parallel, v_\perp, t) = \frac{\partial}{\partial v_\parallel} D_0 \frac{\partial f}{\partial v_\parallel} + \left(\frac{\partial}{\partial v_\parallel} - \frac{v_\parallel}{v_\perp}\frac{\partial}{\partial v_\perp}\right) D_1 \left(\frac{\partial f}{\partial v_\parallel} - \frac{v_\parallel}{v_\perp}\frac{\partial f}{\partial v_\perp}\right) - E\frac{\partial f}{\partial v_\parallel} + \frac{\partial}{\partial v_\parallel}\nu(v_\parallel)\left(v_\parallel f + \frac{\partial f}{\partial v_\parallel}\right) \qquad (1)$$

with

$$D_0(v_\parallel, t) = 2\pi \int_{k_\parallel > 0} \frac{d^3k}{(2\pi)^3}\, \varepsilon(\vec{k}, t)\, \delta\!\left(\frac{k_\parallel}{k} - k_\parallel v_\parallel\right) , \qquad (2)$$

$$D_1(v_\parallel, v_\perp, t) = \frac{\pi}{2} \int_{k_\parallel > 0} \frac{d^3k}{(2\pi)^3} \left(\frac{k_\parallel}{k}\right)^2 \varepsilon(\vec{k}, t) \left(\frac{k_\perp v_\perp}{\omega_{ce}}\right)^2 \delta(\omega_{ce} - k_\parallel v_\parallel) . \qquad (3)$$

Here, E is the applied electric field and the collisions are modeled by a Vedenov[5] term with $\nu(v_\parallel) = \nu_0(1 + v_\parallel^2)^{-3/2}$. Since this term is linear, it simulates situations in which the dissipated energy is removed into a thermal reservoir. On the other hand, this model well describes the randomization of the distribution function toward a Maxwellian, which would be expected to follow the quasi-linear stage, and so is convenient for our purpose. In the units used, E is normalized according to $E \to E(4\pi nT)^{1/2}$, so that the ratio $(\nu_0/E)^{1/2}$ is just the critical velocity v_c above which the electric field dominates the collisional drag and the electrons become runaways. Alternatively, the ratio $2(E/\nu_0)$ may be regarded as the electric field expressed in units of the Dreicer field.

With regard to the evolution of the spectrum we use the equations

$$\frac{\partial}{\partial t}\,\mathcal{E}(\vec{k},t) = 2(\gamma_0 + \gamma_1 - \nu_0/2)\,\mathcal{E}(\vec{k},t) \tag{4}$$

with

$$\gamma_0 = \frac{\pi}{2}\frac{k_\parallel}{k^3}\int d^3v\; k_\parallel \frac{\partial f}{\partial v_\parallel}\,\delta\!\left(\frac{k_\parallel}{k} - k_\parallel v_\parallel\right), \tag{5}$$

and

$$\gamma_1 = \frac{\pi}{8}\frac{k_\parallel}{k^3}\int d^3v \left(\frac{k_\perp v_\perp}{\omega_{ce}}\right)^2 k_\parallel \left(\frac{\partial f}{\partial v_\parallel} - \frac{v_\parallel}{v_\perp}\frac{\partial f}{\partial v_\perp}\right)\delta(\omega_{ce} - k_\parallel v_\parallel)\,. \tag{6}$$

The set of equations (1)-(6) conserves neither energy nor momentum. The electric field term and the Vedenov term act as a source and a sink, respectively, that destroy the momentum balance. In contrast, Eq. (1) is conservative with respect to the number of particles insofar as there is no flux at the boundaries.

Let us consider a distribution function with a runaway tail, and a wave with a wavenumber k. The wave may interact with the distribution in two different regions : the resonant velocity for the Cerenkov interaction $v_\parallel = 1/k$ (denoted by v_r^c), which is smaller than the resonant velocity for the anomalous Doppler interaction $v_\parallel = \omega_{ce}/k_\parallel$ (denoted by v_r^d). Both resonances rapidly scatter electrons in velocity space when the system turns unstable. The anomalous Doppler resonance contributes to the part γ_1 of the total growth rate [eq. (6)]. γ_1 is always positive for a runaway tail and increases with $v_\parallel/v_\perp$; hence, it increases with v_r^d. The scattering associated is nearly elastic ($\omega_{ce} \gg \omega_k$). The electrons are scattered in pitch angle; they lose some longitudinal kinetic energy to the benefit of their gyration energy. In contrast, the part of the growth rate γ_0 due to the Cerenkov resonance is usually negative [eq. (5)]; it has the sign of the derivative of the distribution function and decreases in absolute value as v_r^c increases. The Cerenkov interaction scatters the electrons in energy and acts to produce a plateau on the distribution.

In view of the above comments, there is no one-to-one correspondence between the spectrum and the distribution function. It is therefore useful to introduce the two projectors : $\delta(v_\parallel - k^{-1})$ and $\delta(v_\parallel - \omega_{ce}/k_\parallel)$. They allow us to project the two-dimensional spectrum $\varepsilon(k_\parallel, k_\perp, t)$ onto the velocity subspace $v_\parallel$. For the Cerenkov interaction one obtains

$$I^c(v_\parallel, t) = \int_{k_\parallel > 0} \frac{d^3k}{(2\pi)^3} \, \mathcal{E}(k_\parallel, k_\perp, t) \, \delta(v_\parallel - k^{-1}) \quad . \tag{7}$$

In the case of the anomalous Doppler interaction the projection yields

$$I^d(v_\parallel, t) = \int_{k_\parallel > 0} \frac{d^3k}{(2\pi)^3} \, \mathcal{E}(k_\parallel, k_\perp, t) \, \delta\left(v_\parallel - \frac{\omega_{ce}}{k_\parallel}\right) \quad . \tag{8}$$

Let us note that the total fluctuation energy is equal to

$$W = 2\int_0^\infty dy\, I^c(y) = 2\int_0^\infty dz\, I^d(z) .$$

B. Onset of Langmuir turbulence

From Eq. (4) we see that there are only two ways for an instability to be triggered. Either γ_1 is large enough to overcome the damping due to γ_0 and collisions, or γ_0 itself is also positive. Hitherto, the studies[1,3,6–10] have considered only the first way, and the initial runaway distribution functions used were modeled in some way suggested by the classical asymptotic theory of runaway tails. The tails were given enough particles for the distributions to be unstable with respect to the anomalous Doppler effect, and the development of the instability was studied from this point forward. However, the threshold for instability depends very much on the shape of the distribution. A recent and seemingly more consistent work[11] has shown that for realistic electric fields the runaway distribution is only marginally unstable. Nevertheless, the numerical code used is reliable up to a velocity of the order of 10-15 v_{te} so that the shape of the distribution for higher velocities had to be extrapolated. Thus, the other way of triggering this instability, namely the onset of a positive slope, was missed even though the evolution of a runaway distribution function was followed from an initial Maxwellian. This phenomenon is purely dynamical and has to be understood as such. The initially Maxwellian distribution grows a tail under the influence of an electric field. As the bulk depletes, the flux of electrons through

$v_c = (\nu_0/E)^{1/2}$ tends to diminish. Thus, unless there is a source of electrons below v_c, strong enough to prevent the depletion of the bulk, the flux of electrons that become runaways will decrease in the course of time, which results in the onset of a positive slope on the tail of the distribution function. Of course, in a consistent approach the collective effects, which occur on a much faster time scale than the growth of a runaway tail, will never allow the formation of a true positive slope since the slightest tendency toward a positive slope will be immediately thwarted by the Cerenkov effect. A self-consistent spectrum of electrostatic fluctuations is thus built, together with the runaway tail, which in turn may cause the fastest electrons to diffuse via the anomalous Doppler interaction.

In view of this situation, any consideration of threshold turns out to be unreliable. If we consider the first way, the system is only marginally unstable and any perturbation may destabilize it. If we envisage the second way, the threshold will be completely modified in nature by the role of the source of the electrons. Nevertheless, the instability remains whatever its origin.

C. Development of the instability and partial destruction of the tail

As seen in the previous section, the instability may originate either from anomalous Doppler resonance, or from Cerenkov resonance. The electric field and the Vedenov terms have been introduced in the computer code, already used in Ref. 4, in order to investigate the two corresponding sequences of events. The first sequence is simulated by integrating

Eq. (1) over the half-space $v_\parallel > 0$. We follow the evolution in time of the system described by Eqs. (1) - (6) starting with a Maxwellian for $f(v_\parallel, v_\perp, t=0)$ and thermal noise for $\varepsilon(\vec{k}, t = 0)$. The use of the boundary condition $f(v_\parallel = 0, v_\perp, t) = f(v_\parallel = 0, v_\perp, t = 0)$ prevents the depletion of the bulk and so amounts to introducing a source of particles at $v_\parallel = 0$. However, the system evolves only toward a marginally stable state as explained in Sec. II.B and has to be triggered into the instability domain. The second sequence is simulated by integrating Eq. (1) over the full velocity space $-\infty < v_\parallel < +\infty$. Of course, technically the mesh has a finite size but is chosen broad enough (typically $-8 < v_\parallel < +50$) to avoid fluxes of particles at the boundaries. In this case the distribution function conserves the number of electrons present in the initial Maxwellian.

The two sequences of events differ only during the earlier stages. Since the first case has already been abundantly treated in the literature,[1,3,6-10] here we give the second sequence only, marking the point where it becomes independent of the onset.

As the runaway tail grows, the bulk of the distribution depletes, so that it may not continue to deliver as many electrons to the tail. This shortage would allow a positive slope to appear on the distribution function if the Cerenkov effect did not flatten it immediately. As a result, a spectrum of Langmuir fluctuations, which continuously widens, is built and sustained during the growth of the runaway tail as shown in Fig. 1. At the time of its appearance the spectrum is situated in too high a v_r^c to act on the leading edge of the tail via the anomalous Doppler interaction. In v_r^d the spectrum lies in a region of the velocity space where there are no electrons yet.

Nevertheless, the tail stretches with time so its head reaches the edge of the spectrum. From this moment forward the characteristic time scale of the events is dramatically reduced (Fig. 2). As derived in Appendix A, the reduction factor is roughly $30\ \omega_{ce}\nu_0(E/\nu_0)^{3/2}\exp(\nu_0/4E)$. The electrons in the head are then scattered by the anomalous Doppler interaction and the runaway tail stops growing. Simultaneously, there is a strong enhancement of the waves with the smallest v_r^c, because they become unstable both for the Cerenkov and anomalous Doppler effects. As a result, a true plateau appears in the corresponding region of the distribution function and the associated backward flux allows the extension of the spectrum toward even smaller v_r^c.

More electrons are then pitch-angle scattered via the anomalous Doppler interaction, which leads to a shrinking of the tail together with an increase in the local perpendicular temperature. The slope of the distribution function, integrated over $v_\perp$, then becomes sufficiently positive again to destabilize the plasma waves via the Cerenkov effect.A backward flux pushes the electrons with high gyration energy down to the bulk, which results in an increase of the perpendicular temperature and of the level of turbulence all along the tail (Fig. 3).

From this stage forward the two sequences mingle irrespective of the initial condition for the instability (cf. Sec. II B). Moreover, it turns out that the electric field and the collisions may be completely neglected for a while; the "non-elastic isotropization" described in Ref. 4 takes place. Thus, the tail is destroyed little by little.

In the case of an electron beam, the end of the relaxation is characterized by two edge points C and D taking up their final positions.[4] In the present problem the electric field and the collisions play a role and determine the position of C as being equal to the critical velocity v_c. Once the positions of C and D are fixed, the fluctuations are damped by the collisions and their energy drops down by a few orders of magnitude (cf. Fig. 2). However, they do not disappear into the thermal noise. The system reaches a very stable state, far from thermodynamic equilibrium, which is sustained by a flux of energy going from the electric field into the thermal reservoir. The shape of the distribution function as well as the projections of the spectrum $I^c(v_\parallel)$ and $I^d(v_\parallel)$ are shown in Fig. 4. The distribution displays a very small positive slope between C and D; the corresponding backward flux due to the Cerenkov effect balances the acceleration of the electrons due to the electric field. Beyond D the distribution function sharply decreases with the degree of anisotropy that is needed to convert the work done on the electrons by the electric field into gyration energy. Figure 5 displays the two-dimensional spectrum; the dashed lines indicate the fluctuations excited mainly by the Cerenkov effect while the dotted lines indicate those mainly due to the anomalous Doppler effect.

III. THE QUASI-STATIONARY STATE

A. A non-Maxwellian attractor for the distribution function

One of the essential features of the distribution of the runaways at the time of the instability is the backward flux of the electrons. The backward diffusion is associated with the small positive slope that originates from the shrinkage of the tail by the anomalous Doppler effect.

This phenomenon was overlooked in the model proposed by Parail and Pogutse.[1] Moreover, in the moment equations, they modeled the Cerenkov interaction ad hoc by a term that implies a negative slope a priori. From our computations, however, it turns out that after the burst the distribution function maintains the positive slope needed for the backward diffusion to balance the electric field acceleration. Thus, the periodicity described by the moment equations is an artefact due to their excessive stiffness. In fact, the shape of the distribution function is flexible enough to adapt the time scale of the turbulence to that of the electric field. The quasi-stationary state found displays a remarkable stability. Different numerical attempts were made in order to impede the proper development of the burst by introducing extra damping effects, selective or non-linear, in the wave equation. Yet in all cases the distribution function evolved toward the quasi-stationary solution while the history remains hidden in the details of the final spectrum. Here, we wish to bring to attention an inconsistency that affects all the works published so far on the subject. During the burst the high value of the ratio between fluctuations and kinetic energy indicates that the role of the non-resonant interaction should be taken into account. However, after having studied cases with an extra nonlinear damping, we are convinced that a proper account of the non-resonant interaction might moderately affect the history of the burst but certainly not the final quasi-steady state found. It should be mentioned that other authors[12] have already proposed a stationary model for a runaway distribution including collective effects. However, contrary to the results presented here, no consideration of the stability is used to support their stationary solution. In fact, a comparison is difficult because, as distinct from Ref. 12, our work lies in the commonly adopted frame of a homogeneous plasma. There is no link, in spite of appearances, between $D = \omega_{ce}\ C$ and the point p_c of Ref. 12, since it is defined as the lowest edge of the spectrum in v_r^d and not as the point where a friction due to the anomalous Doppler effect could balance the electric field acceleration.

On the other hand, we do not claim that there exists a true stationary state. The flux of electrons driven by the electric field through the critical velocity (equal to C) does not vanish because of the turbulence. Simply, the runaway electrons are blocked in the region between C and D so that the state lasts for the time of the order of the runaway production time $\tau = (\nu_0/E)^{3/2}\ \exp(\nu_0/4E)\ \nu_0^{-1}$ (cf. Appendix A). The crucial point is that this time is much longer than the collisional time, typically by a factor of 10^4. Therefore, this time has nothing to do with the period of the relaxations observed in tokamaks.[2]

Thus, what we claim is that, after one burst, the system described by the equations used in Refs. 1, 3, 6-10 evolves toward a quasi-steady, very stable and turbulent state; the system is not recycled to a state from which the instability could grow up again. The problem of the additional physical mechanism which causes the periodicity observed in many experiments is still open.

Let us now turn to the analytical description of the quasi-steady state.

B. Analytical model

To the accuracy of the runaway production rate which is[8] $A = \nu_0(E/\nu_0)^{3/2}\exp(-\nu_0/4E)$ we may drop the time derivative in Eq. (1):

$$+E\frac{\partial f}{\partial v_{\parallel}} - \frac{\partial}{\partial v_{\parallel}}\nu(v_{\parallel})\left(v_{\parallel} f + \frac{\partial f}{\partial v_{\parallel}}\right) = \frac{\partial}{\partial v_{\parallel}} D_0 \frac{\partial f}{\partial v_{\parallel}} + \left(\frac{\partial}{\partial v_{\parallel}} - \frac{v_{\parallel}}{v_{\perp}}\frac{\partial}{\partial v_{\perp}}\right) D_1 \left(\frac{\partial f}{\partial v_{\parallel}} - \frac{v_{\parallel}}{v_{\perp}}\frac{\partial f}{\partial v_{\perp}}\right).$$

This equation is simplified by introducing the Maxwellian ansatz discussed in Ref. 4

$$f(v_{\parallel}, v_{\perp}, t) = F(v_{\parallel}, t)\,\frac{1}{2\pi\, T_{\perp}(v_{\parallel}, t)}\exp\left(-\frac{1}{2}\frac{v_{\perp}^2}{T_{\perp}(v_{\parallel}, t)}\right).$$

It reduces to an ordinary differential equation for F(v,t) where the variable v signifies $v_{\parallel}$ and t is a parameter

$$+E\frac{\partial F}{\partial v} - \frac{\partial}{\partial v}\nu(v)\left(vF + \frac{\partial F}{\partial v}\right) = \frac{\partial}{\partial v}\left[D_0\frac{\partial F}{\partial v} + \bar{D}_1\left(\overline{\frac{\partial}{\partial v}(T_{\perp}F) + vF}\right)\right]. \tag{9}$$

Here

$$D_0(v) = \frac{1}{2\pi}\int_0^{\pi/2} d\varphi \int_0^{\infty} dk\, k\sin\varphi\cos\varphi\, \varepsilon(\vec{k})\,\delta\left(\frac{1}{k} - v\right), \tag{10}$$

$$\bar{D}_1(v) = \frac{1}{4\pi} \int_0^{\pi/2} d\varphi \int_0^{\infty} dk\, k^4 \sin^3\varphi \cos^2\varphi \frac{1}{\omega_{ce}^2} \mathcal{E}(\vec{k}) \, \delta(\omega_{ce} - kv\cos\varphi) \,, \tag{11}$$

and $\nu(v) = \nu_0(1 + v^2)^{-3/2}$ follow straightforwardly from the full equations (1) - (3).

As for the spectrum, Eqs (4) - (6) become

$$2\gamma_0 + 2\gamma_1 - \nu_0 = 0 \,, \tag{12}$$

with

$$\gamma_0 = \frac{\pi}{2} \frac{\cos\varphi}{k^2} \int dv \, \frac{\partial F}{\partial v} \, \delta\left(v - \frac{1}{k}\right) \,, \tag{13}$$

and

$$\gamma_1 = \frac{\pi}{4} \frac{\sin^2\varphi \cos\varphi}{\omega_{ce}^2} \left[\frac{\partial}{\partial v}(T_\perp F) + \frac{\omega_{ce}}{k\cos\varphi} F \right] \Bigg|_{v = \frac{\omega_{ce}}{k\cos\varphi}} \,. \tag{14}$$

On the one hand, we divide the velocity space into three regions corresponding to the three different mechanisms that may thwart the acceleration of the electrons by the electric field; the spectrum on the other hand is separated into two parts depending on the emission mechanism. The characteristic points of the model C and D are reported in Figs. 4 and 6. C is the lowest edge of the spectrum in v_r^c; for lower velocities (region I) the distribution function is determined by the electric field and the collisions only. Besides, we assume that at a point L the spectrum may be separated into two parts; for $v_r^c < L$, it is excited by the anomalous Doppler interaction with the electrons in region III (beyond D); for $L < v_r^c < D$ it is maintained, via the Cerenkov effect, by a small positive slope on the distribution function.

Let us now solve Eqs. (9) - (14) for the distribution function and for the spectrum. We start from region III in this way following the backward flux from its origin. It is worth recalling the dominant character of the Cerenkov effect over the anomalous Doppler effect, already noted in Ref. 4. For this reason, the perpendicular spread of the tail may be considered as uniform wherever the Cerenkov effect may interfere, namely, from C upward.

In region III, v > D, we balance the flux due to the electric field with the backward flux caused by the anomalous Doppler interaction

$$E F = \bar{D}_1 \left(T_\perp \frac{\partial F}{\partial v} + v F \right) , \qquad v > D . \tag{15}$$

The distribution function has just the degree of anisotropy necessary to maintain the level of the fluctuations in part I of the spectrum ($C < v_r^c < L$).

The latter is assumed to have the shape

$$\mathcal{E}(\vec{k}) = \delta(k - k_0)\,\bar{\mathcal{E}}_1(\varphi) \tag{16}$$

where

$$c < k_0^{-1} < L .$$

With this ansatz, the diffusion coefficient D takes the form

$$\bar{D}_1(v) = \frac{1}{4\pi}\frac{k_0^3}{\omega_{ce}^2}\left[1 - \left(\frac{\omega_{ce}}{k_0 v}\right)^2\right]\left(\frac{\omega_{ce}}{k_0 v}\right)^2 \frac{1}{v}\,\bar{\mathcal{E}}_1\left[\varphi = \arccos\left(\frac{\omega_{ce}}{k_0 v}\right)\right] , \quad v > D . \tag{17}$$

The part of Eq. (15) that implies the shape of the distribution function may be evaluated by means of the marginal stability condition $2\,\gamma_\perp = \nu_0$. This is written in v space via the resonance condition $v = \omega_{ce}/k_0 \cos\varphi$

$$\left(T_\perp \frac{\partial F}{\partial v} + v F\right)\left(\frac{\omega_{ce}}{k_0 v}\right)\left[1 - \left(\frac{\omega_{ce}}{k_0 v}\right)^2\right] = 2\,\frac{\omega_{ce}^2}{\pi}\,\nu_0 , \quad v > D . \tag{18}$$

Now we are able to solve Eq. (15) for the spectrum

$$\bar{\mathcal{E}}_1\left[\varphi = \arccos\left(\frac{\omega_{ce}}{k_0 v}\right)\right] = \frac{2\pi^2}{\omega_{ce}}\frac{E}{\nu_0}\frac{1}{k_0^2}\,v^2 F(v) , \quad v > D . \tag{19}$$

Since ν_0 is small in Eq. (18), it is reasonable to approximate F(v) by the isotropic distribution

$$F(v) = F(D) \exp\left(-\frac{v^2 - D^2}{2T_\perp}\right), \quad v > D \tag{20}$$

In region II, $c < v < D$, we balance the flux due to the electric field with the backward flux caused by the Cerenkov interaction:

$$EF = D_0 \frac{\partial F}{\partial v}, \quad C < v < D. \tag{21}$$

As we shall see, D_0 is much larger than E so that as a first approximation

$$F(v) = F(D) = F(C), \quad C < v < D. \tag{22}$$

However, to get part II of the spectrum ($L < v_r < D$), Eq. (21) is solved for $D_0(v)$ with the shape given by the marginal stability condition $2\ \gamma_0 = \nu_0$. For the most unstable, parallel waves the latter reads

$$v^2 \frac{\partial F}{\partial v}(v = k^{-1}) = \frac{1}{\pi}\nu_0, \quad L < v < D$$

Substituting this expression into Eq.(21), we obtain

$$D_0(v) = \pi \frac{E}{\nu_0} v^2 F(C), \quad L < v < D, \tag{23}$$

where Eq. (22) was used.

We assume part II of the spectrum to have the shape

$$\mathcal{E}(\vec{k}) \begin{cases} = \bar{\mathcal{E}}_2(k) & \text{for } 0 < \varphi < \phi, \\ = 0 & \text{otherwise,} \end{cases} \tag{24}$$

so that Eq(10) takes the form

$$D_\circ(v) = \frac{1}{4\pi}(1 - \cos^2\phi)\frac{1}{v^3}\bar{\mathcal{E}}_2(k = 1/v)$$

which is compared with Eq. (23) to give

$$\bar{\mathcal{E}}_2(k = 1/v) = \frac{4\pi^2}{1 - \cos^2\phi}\frac{E}{\nu_\circ}v^5 F(c), \quad L < v < D. \tag{25}$$

In region I, $-\infty < v < C$, the Coulomb collisions balance the electric field so that Eq. (9) reduces to

$$E\frac{\partial F}{\partial v} = \frac{\partial}{\partial v}\left[\frac{\nu_\circ}{(1 + v^2)^{3/2}}\left(v F + \frac{\partial F}{\partial v}\right)\right].$$

Due to the boundary condition $F(v = -\infty) = 0$, this equation remains homogeneous after the first integration. The second integration yields

$$F(v,t) = \mathcal{H}(t)\left(\frac{(1 + v^2)^{1/2} + v}{(1 + v^2)^{1/2} - v}\right)^{3E/16\nu_\circ}$$
$$\exp\left[-\frac{v^2}{2} + \frac{E}{4\nu_\circ}v(1 + v^2)^{1/2}\left(v^2 + \frac{5}{2}\right)\right], -\infty < v < C, \tag{26}$$

where $\mathcal{H}$ is determined either by the condition $\int_{-\infty}^{+\infty} dvF(v) = 1$ or by the condition $F(v = o) = (2\pi)^{-1/2}$, depending on the model assumed (cf. the two sequences in Secs. IIB and C).

It is interesting to note that this expression displays a minimum at $v = v_C$ beyond which it increases monotonically. The Cerenkov effect would not allow such a distribution and so necessarily $C \leq v_C$. On the other hand, since for $v < v_C$, the collisions are strong enough to compete with the electric field, they are a fortiori able to compete the turbulence originating from it and to recreate a negative slope on the distribution function. Thus, it is logical to choose $C = v_C$, which is compatible with the situation at the end of the relaxation (cf. Sec. IIC).

As for the perpendicular temperature $T_\perp(v,t)$, at C it has a high value $T_\perp$ imposed from the right by the collective effects and in region I it is determined by the collisional diffusion toward the bulk. Since F(C) is determined by the matching condition for the distribution function at C, $T_\perp$ is the only degree of freedom remaining in the model. Its value depends, of course, on the extension of the tail at the onset of the burst, and thus is closely related to the problem of threshold for the instability discussed in Sec. IIB. On the other hand, $T_\perp$ increases slowly but continuously during the quasi-steady state at the same rate as the anomalous Doppler interaction diffuses the electrons in region III.

Thus, $\bar{T}_\perp(t)$ consists of two parts

$$\bar{T}_\perp(t) = \bar{T}_\perp^\circ + \Delta T_\perp(t) \quad ,$$

where $\bar{T}_\perp^o$ (cf. Appendix B) is the value attained at the end of the burst and is determined by the history of the instability; $\Delta T_\perp(t)$ is the increment added during the quasi-steady state. Let us show how this increment is determined within the frame of our model.

In view of the approximation of elastic scattering of the particles via the anomalous Doppler effect, the power delivered by the electric field to the electrons in region III is equal to the gain of gyration energy per unit of time

$$\frac{d}{dt}\left(K_\perp\right) = E \int_D^\infty dv\, v\, F(v) = E\, F(c)\, \bar{T}_\perp \quad . \tag{27}$$

Besides, we may simply write $K_\perp$ as $\bar{T}_\perp$ times the number of particles in thetail so that

$$\frac{d}{dt}\left(K_\perp\right) = F(c)\left[\dot{\bar{T}}_\perp\,(D-c) + 2\,\frac{\bar{T}_\perp}{D}\dot{\bar{T}}_\perp\right] \quad ,$$

where the dots mean the derivatives with respect to time.

Hence,

$$\frac{\dot{\bar{T}}_\perp}{\bar{T}_\perp}\,(D-c) + \frac{2}{D}\,\dot{\bar{T}}_\perp = E \quad .$$

By integrating this equation with the initial condition $\bar{T}_\perp(t = o) = \bar{T}_\perp{}^\circ$,

one obtains

$$Et = (D-C)\,\ln\left(\frac{\bar{T}_\perp}{\bar{T}_\perp^\circ}\right) + \frac{2}{D}\left(\bar{T}_\perp - \bar{T}_\perp^\circ\right) \quad . \tag{28}$$

Now, since the increase in the perpendicular spread during the quasi-steady state is a slow process, we assume $\Delta T_\perp/\bar{T}_\perp{}^o \ll 1$. Then, Eq. (28) yields

$$\Delta T_\perp(t) = \frac{\bar{T}_\perp^\circ\, D\, E}{2\bar{T}_\perp^\circ + C^2(\omega_{ce}-1)}\, t$$

$$\Delta T_\perp(t) \cong \frac{DE}{2}\left(1 - \frac{C^2(\omega_{ce}-1)}{2\,T_\perp^\circ}\right) t \;,$$

which is in agreement with our computational experiments.

One of the important results presented in this paper is the quasi-steady turbulence. Let us show how the analytical model yields simple formulae to estimate the level of turbulence from the values of the parameters E, ν_o, and ω_{ce}.

The part of the spectrum excited by the Cerenkov effect (part II) contains the energy

$$W_2 = 2\int \frac{d^3k}{(2\pi)^3}\, \mathcal{E}(\vec{k}) = \left(\frac{1-\cos\phi}{2\pi^2}\right)\int k^2 dk\; \bar{\mathcal{E}}_2(k) \quad .$$

On performing the transformation v = 1/k in the last integral and substituting $\bar{\mathcal{E}}_2(k)$ from Eq. (25), one obtains

$$W_2 = \frac{2}{1+\cos\phi} F(D) \frac{E}{\nu_0} \int_L^D v\, dv \quad . \tag{29}$$

On comparing this expression with Eq. (7), we note that the projection $I^c(v)$ is linear in v. This is consistent with the numerical results reported in Fig. 4. Using the approximations $\phi \to 0$, $L \to C$, Eq. (29) may be written as

$$W_2 = \frac{E}{\nu_0} F(C) \frac{D^2 - C^2}{2} = \frac{1}{2} F(C) \left(\omega_{ce}^2 - 1\right) \quad . \tag{30}$$

This expression offers a simple interpretation: The work done by the electric field on the electrons in region II is transformed into the fluctuation energy W_2 which in turn is dissipated via collisions in the bulk.

The part of the spectrum due to anomalous Doppler effect (part I) contains the energy

$$W_1 = 2 \int \frac{d^3k}{(2\pi)^3} \mathcal{E}(\vec{k}) = \frac{k_0^2}{2\pi^2} \int d(\cos\varphi)\, \bar{\mathcal{E}}_1(\varphi)$$

that we rewrite in the variable $v = \omega_{ce}/k_0 \cos\varphi$. Using Eq. (19) one obtains

$$W_1 = \frac{1}{k_o} \frac{\bar{E}}{\nu_o} \int_D^{\infty} F(v)\, dv \quad .$$

On introducing the isotropic approximation, Eq. (20), we find

$$W_1 = \frac{1}{k_o} \frac{E}{\nu_o} F(D) \frac{\bar{T}_\perp}{D} \quad . \tag{31}$$

Again, in the limit $L \to C$, we have $k_o\ D = D/C = \omega_{ce}$ and Eq. (31) may be written as

$$W_1 = \frac{E}{\nu_o} F(C)\, \bar{T}_\perp \frac{1}{\omega_{ce}} = \frac{E}{\nu_o} \frac{1}{\omega_{ce}} \int_D^{\infty} v\, F(v)\, dv \quad . \tag{32}$$

Here, it should be recalled that, in the case of a magnetized plasma, the energy of the plasmon emitted via the anomalous Doppler effect is negligible compared with kinetic energy transfer in the pitch-angle scattering. Within this approximation the amount of energy which is not conserved (energy in the fluctuations) scales as $(\omega_{ce})^{-1}$ times the kinetic energy transfer. In comparison with Eq. (27), Eq. (32) simply expresses that the amount of power not conserved is $(\omega_{ce})^{-1}\ dK_\perp/dt$, namely, the part which goes into the fluctuations and is ultimately dissipated in the thermal reservoir. The formulae (30) and (32) are found to be in fairly good agreement with the computational results. Moreover, they are very simple to use. Apart from the value of $\overline{T}_\perp$ which, in principle, is given by the history, all the quantities involved may be evaluated by means of the expressions displayed in this section. Often one may do without the value of $\overline{T}_\perp$ insofar as the number of particles beyond D is small; hence, $W_1 < W_2$. Moreover, $\overline{T}_\perp^\circ$ may be estimated, if necessary, by a formula given in Appendix B. It might be surprising that the two formulae yield values which seem relatively high at first glance. However, it should not be forgotten that they are measured in units of the initial kinetic energy which is much less than the final one. Thus, in the spirit of quasi-linear theory, they should be renormalized to the actual kinetic energy; this operation has been performed for I^c and I^d in Figs. 1, 3, and 4.

IV. MACROSCOPIC EFFECTS

By way of application one may use the analytic model to calculate the current and the fluxes associated with the trapped electrons.

A. Current and conductivity

The first moment of the distribution function $\int_{-\infty}^{+\infty} vF(v)dv$ consists of three distinct parts. The first contribution is written by means of Eq. (26), conveniently simplified:

$$\langle v \rangle_1 = \int_{-\infty}^{c} \mathcal{H}\, v \exp\left[-\frac{v^2}{2} + \frac{1}{4}\frac{E}{\nu_0} v(1+v^2)^{5/2}\left(v^2 + \frac{5}{2}\right)\right] dv .$$

The second contribution is due to the flat domain of the distribution function

$$\langle v \rangle_2 = \int_C^D F(C)\, v\, dv = F(C)\, \frac{C^2}{2} \left(\omega_{ce}^2 - 1\right) \quad ,$$

where the relation $D = \omega_{ce}\ C$ has been used. The third contribution is evaluated using Eq. (20)

$$\langle v \rangle_3 = \int_D^\infty F(D) \exp\left(-\frac{v^2}{2T_\perp}\right) v\, dv = F(C)\ T_\perp \ ,$$

where $T_\perp$ may be estimated via the formula proposed in Appendix B. For $\omega_{ce} \sim 3$ and E/ν_0 within the range 6% - 12%, the first contribution is negligible compared with the others, so that it is possible to write the formula for the conductivity as

$$\sigma = \frac{\langle v \rangle_2 + \langle v \rangle_3}{4\pi E}$$

$$\sigma = F(C) \left(\frac{\nu_c}{E}\right)^2 \left\{ \frac{\omega_{ce}^2 - 1}{2} + \omega_{ce}^2 \left[0.5 \exp(0.4 C) - 1\right] \right\} \frac{1}{4\pi \nu_0} \quad ,$$

where the relation $C = v_c = (\nu_0/E)^{1/2}$ has been used.

The correction factor to the classical conductivity $[(4\pi\ \nu_0)^{-1}$ in our units$]$ is a complicated function of the applied electric field and enhances the conductivity typically by one order of magnitude. For example, with $E/\nu_0 = 8\%$ and $\omega_{ce} = 3$ we obtain a factor 50, as in our numerical calculations.

B. Particles trapped in the ripples of the magnetic field

During the quasi-steady state there are energetic electrons near C with a large pitch-angle that can be trapped in the local magnetic mirrors and leave the system with the toroidal drift $v_d = v_\perp^2/2R\omega_{ce}$. Let us try to use our knowledge of the distribution function between C and D to estimate the number of trapped electrons and the associated fluxes.

From Eq. (22) and the Maxwellian ansatz defined at the beginning of Sec. IIIB, one estimates the fraction of trapped electrons as

$$n_{tr} = \int_C^D dv_\parallel \int_{v_\parallel \delta}^{\infty} dv_\perp \frac{v_\perp}{\bar{T}_\perp} \exp\left(-\frac{v_\perp^2}{2\bar{T}_\perp}\right) F(c)$$

$$n_{tr} \cong F(c) \frac{\bar{T}_\perp}{c\,\delta^2} \exp\left(-\frac{c^2\delta^2}{2\bar{T}_\perp}\right)$$

where $\delta = (B/2\delta B)^{1/2}$.

In the same way one estimates the flux of drifting electrons

$$\phi_d = \int_C^D dv_\parallel \int_{v_\parallel \delta}^{\infty} dv_\perp \frac{v_\perp^3}{\bar{T}_\perp} \exp\left(-\frac{v_\perp^2}{2\bar{T}_\perp}\right) \frac{F(C)}{2R\,\omega_{ce}}$$

$$\phi_d \cong \frac{\bar{T}_\perp}{2R\omega_{ce}} F(C)\left(C + 3\frac{\bar{T}_\perp}{C\delta^2}\right) \exp\left(-\frac{C^2\delta^2}{2\bar{T}_\perp}\right),$$

and the associated flux of energy

$$\phi_e = \int_C^D dv_\parallel \int_{v_\parallel \delta}^{\infty} dv_\perp \frac{v_\perp^4}{\bar{T}_\perp} \exp\left(-\frac{v_\perp^2}{2\bar{T}_\perp}\right) \frac{F(C)}{4R\,\omega_{ce}}$$

$$\phi_e \cong \frac{\bar{T}_\perp}{4R\omega_{ce}} F(C)\left(\delta^2C^3 + 7\bar{T}_\perp C + 15\frac{\bar{T}_\perp^2}{C\delta^2}\right) \exp\left(-\frac{\delta^2C^2}{2\bar{T}_\perp}\right).$$

For typical tokamak parameters, $E/\nu_o \simeq 0.1$, $\omega_{ce}/\omega_{pe} \simeq 3$, $R/\lambda_D \simeq 10^4$, and $\delta \simeq 10$, we find in succession $n_{tr} \simeq 6\ 10^{-6}$, $\phi_d \simeq 1\ 10^{-7}$, $\phi_e \simeq 7\ 10^{-5}$; in physical units $\phi_e \simeq 100$ W/cm^2 for a plasma temperature of 1 keV.

V. CONCLUSION

We have studied the dynamics of the formation and destruction of the runaway tail together with the self-consistent spectrum of fluctuations generated. The roles of the electric field and Coulomb collisions, as well as the quasi-linear Cerenkov and anomalous Doppler interactions, were taken into account simultaneously without any separation of the different time scales involved.

Instead of periodic relaxations, we have found that after one burst the time scale of the turbulence adapts itself to that of the electric field, which leads to a quasi-steady and very persistent state. It turns out that the backward diffusion of the electrons due to the Cerenkov interaction plays an essential role: it is simply its neglect that introduces the periodicity of the relaxations predicted in Refs. 1 and 3. Also, our self-consistent calculations of the formation of the runaway tail have shown that the notion of a precise instability threshold is questionable. The depletion of the bulk caused by the growth of the tail may or may not be prevented by a source of particles. In the first case, we have found, in agreement with a recent work,[11] that the distribution is only marginally unstable and so has to be triggered into the instability domain. In the second case, we have exhibited a purely dynamical phenomenon that causes, via the Cerenkov interaction, the growth of fluctuations which help the instability to develop.

In spite of the uncertainty tied to the onset of the turbulence, the system always evolves toward the quasi-steady state. This feature led us to develop a simple theoretical model. The state, which appears highly non-Maxwellian, is sustained by a flux of energy originating from the work done by the electric field on the electrons (cf. Fig. 6). While for the low velocity electrons of region I ($v_{\parallel} < C$) the work is directly dissipated into the thermal reservoir for the runaway electrons ($v_{\parallel} > C$) the quasi-linear interactions act as intermediate convertors of the work. For the high velocity electrons of region III ($v_{\parallel} > D$) the work is converted via the anomalous Doppler interaction into gyration energy and into the energy of Langmuir fluctuations. For the intermediate velocity electrons of region II ($C < v_{\parallel} < D$) the work is converted via the Cerenkov interaction into the energy of Langmuir fluctuations. The fluctuations are then damped and their energy dissipated into the thermal reservoir. Due to the cooperation of the two quasi-linear interactions, a suprathermal level of turbulence as well as a non-Maxwellian shape of the electron distribution function is maintained.

Acknowledgments

The authors wish to thank Prof. C.S. Liu for fruitful discussions and Drs. P.D. Morgan and M.L. Sawley for reading the manuscript.

This work was partially funded by the Swiss National Science Foundation and Euratom.

APPENDIX A :

VARIOUS TIME SCALES OF THE PROCESS

The evolution of the quasi-linear equations [Eqs. (1)-(6)] involves at least four different time scales. First, there is a time for building a runaway tail which may be estimated as $\tau_t \sim \nu_0^{-1}(\nu_0/E)^{3/2}$. Secondly, there is a time of the burst which may be estimated via the growth rate for the anomalous Doppler effect $\tau_s \sim 10\ \gamma_1^{-1}$. Using Eq. (14) for the optimum angle one obtains roughly $\tau_s \sim 30\ \omega_{ce}\ (v\ F)^{-1}$ that may be evaluated at $v = v_c\ \omega_{ce}$ by means of the asymptotic runaway distribution given in Ref. 8 to yield $\tau_s \sim 30\ \omega_{ce}\ \exp(\nu_0/4E)$. Thirdly, there is a time of the relaxation toward the quasi-stationary state which scales as (cf. Fig. 2) $\tau_r \sim \nu_0^{-1}$. Finally, there is a time of duration of the quasi-steady state that may be roughly estimated as the inverse of the runaway production rate. Again using a formula given in Ref. 8, one obtains $\tau_q \sim \nu_0^{-1}(\nu_0/E)^{3/2}\ \exp(\nu_0/4E)$. This time may still be larger in current experiments due to the value of Z_{eff}.

APPENDIX B :

ESTIMATE OF $\bar{T}_{\perp}^{o}$

In the case where the instability originates from the positive slope on the distribution function, one may attempt to determine the perpendicular temperature attained at the end of the burst by means of formula (17) given in Ref. 4: $T_{\perp} = D(v_b - D)$.

The beam velocity may be estimated as $v_b = [(\omega_{ce}+1)/2]v_s \simeq (\omega_{ce}/2)v_s$, where v_s is the velocity at which the positive slope appears on the distribution function while growing the runaway tail. Now a simple numerical parameter study allows us to propose the empirical formula

$$v_s = v_c \exp(0.4\, v_c)$$

Thus, one obtains

$$\bar{T}_{\perp}^{o} = D^2 \left(0.5 \exp(0.4\, v_c) - 1 \right) .$$

References

[1] V.V. Parail and O.P. Pogutse, Fiz. Plazmy 2, 228 (1976) [Sov. J. Plasma Phys. 2, 126 (1976)].

[2] P. Brossier, Nucl. Fusion 18, 1069 (1978).

[3] D.-I. Choi and W. Horton, Plasma Phys. 20, 903 (1978).

[4] L. Muschietti, K. Appert, and J. Vaclavik, Phys. Fluids, 24, 151 (1981).

[5] A.A. Vedenov, Theory of Turbulent Plasma. (London Iliffe Book, London, 1968).

[6] K. Papadopoulos, B. Hui, and N. Winsor, Nucl. Fusion 17, 1087 (1977).

[7] C.S. Liu, Y.C. Mok, K. Papadopoulos, F. Engelmann, and M. Bornatici, Phys. Rev. Lett. 39, 701 (1977).

[8] V.V. Parail and O.P. Pogutse, Nucl. Fusion 18, 303 (1978).

[9] C.S. Liu and Y. Mok, Phys. Rev. Lett. 38, 162 (1977).

[10] B.H. Hui and N. Winsor, Phys. Fluids 21, 940 (1978).

[11] J.C. Wiley, D.-I. Choi, and W. Horton, Phys. Fluids 23, 2193 (1980).

[12] K. Molvig, M.S. Tekula, and A. Bers, Phys. Rev. Lett. 38, 1404 (1977).

Figure Captions

Fig. 1:

Typical electron distribution function and spectrum at the onset of turbulence. The distribution looks flat since its tendency to build up a positive slope is continously quenched by the Cerenkov effect. The two-dimensional spectrum is represented by the two projections defined in Eqs. (7) and (8). The area under the curve I^c (or I^d) yields directly the fluctuation energy measured in units of the actual kinetic energy. The parameters used are: $E/\nu_0 = 8\%$, $\omega_{ce} = 3$.

Fig. 2:

Time evolution of the kinetic K, perpendicular kinetic $K_\perp$, and fluctuation energy W. A typical long time evolution is displayed at the top. The total kinetic energy increases monotonically except for the instant of the burst where a part is shared temporarily with the fluctuations. At this instant the perpendicular kinetic energy exhibits a sudden rise and a sharp spike appears in the fluctuation energy. W then relaxes to the quasi-steady value while K increases slowly. K, $K_\perp$, and W, respectively, are equal to 5, 4, and 0.1 times the numbers indicated on the ordinate axis. In the bottom the temporal behavior of the burst is detailed by a factor of 400. The parameters used are: $E/\nu_0 = 8\%$, $\omega_{ce} = 3$.

Fig 3:

Typical electron distribution function and spectrum during the burst. The fully-excited two-dimensional spectrum is projected twice: I^c (dashed line) covers the domain of interaction via the Cerenkov resonance while I^d (dotted line) covers the domain of interaction via the anomalous Doppler resonance. The parameters used are: $E/v_o = 8\%$, $\omega_{ce} = 3$.

Fig. 4:

Typical electron distribution function and spectrum during the quasi-steady state. The shortened tail of the distribution has a small positive slope (not visible) between C and D = ω_{ce} C. The representation of the spectrum and the parameters used are the same as Fig. 3

Fig. 5:

Typical spectrum during the quasi-steady state as obtained from the numerical computations. The dashed lines indicate the waves driven mainly by the Cerenkov effect while the dotted lines indicate those driven by the anomalous Doppler effect. The parameters used are: $E/v_o = 8\%$, $\omega_{ce} = 3$.

Fig. 6:

Schematic diagram of the energy fluxes involved in the quasi-steady state.

FIG. 1

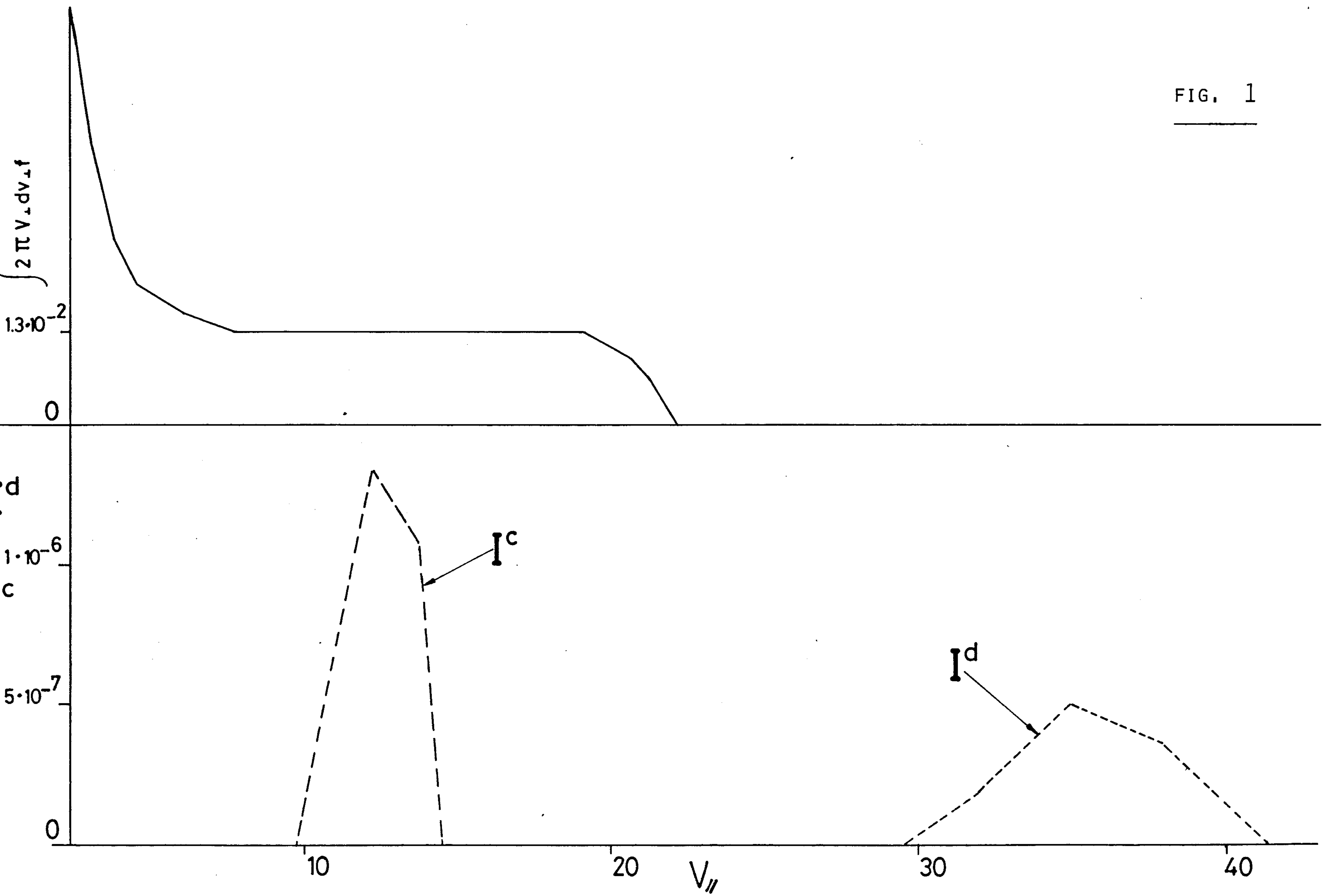

$\int 2\pi v_\perp dv_\perp f$
$1.3\cdot10^{-2}$
0
d
$1\cdot10^{-6}$
c
$5\cdot10^{-7}$
0
I^c
I^d
10
20
30
40
$V_{\parallel}$

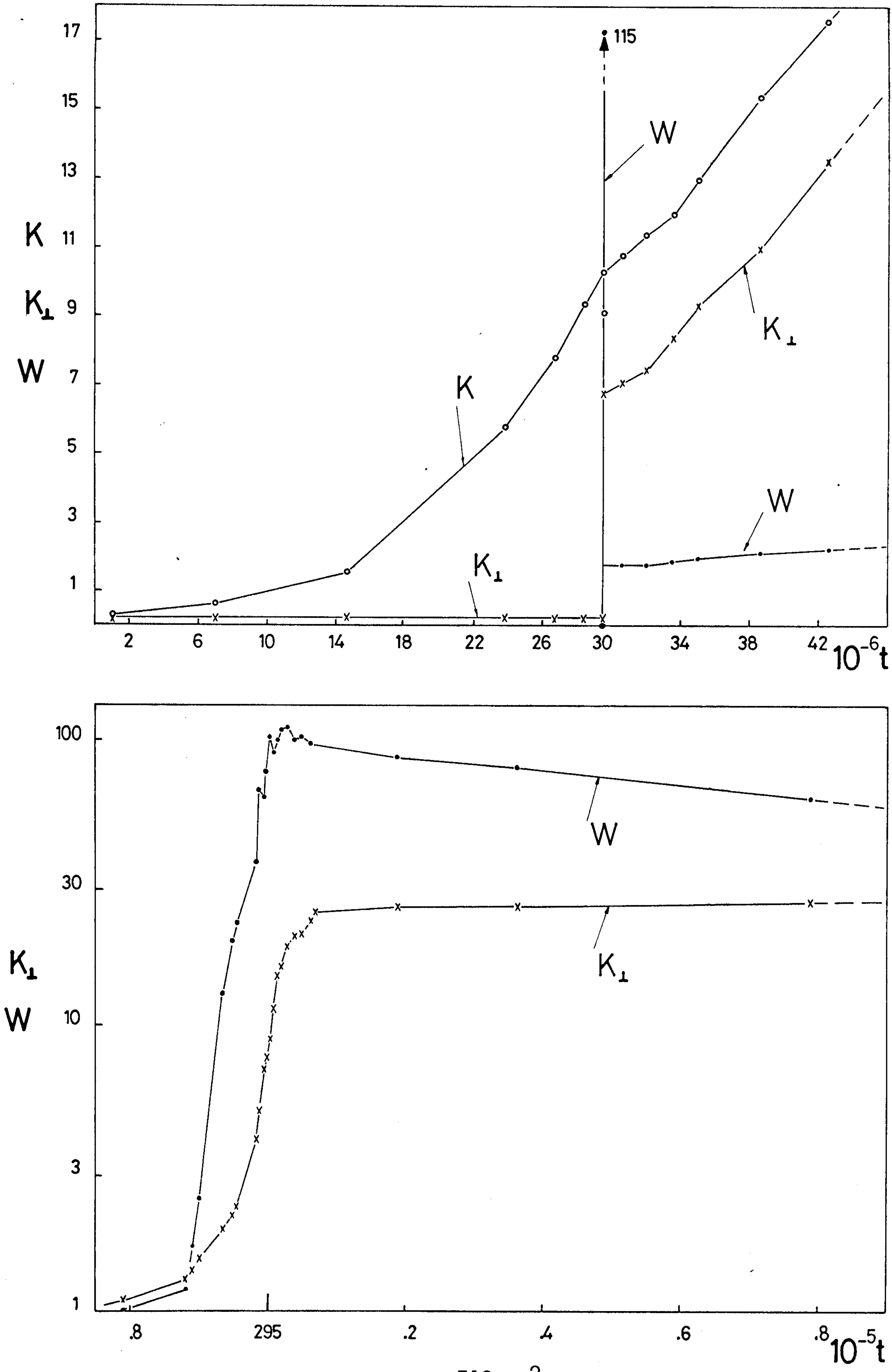

K
K⊥
W
17
15
13
11
9
7
5
3
1
115
W
K
K⊥
W
K⊥
2
6
10
14
18
22
26
30
34
38
42
10⁻⁶t
100
30
10
3
1
W
K⊥
.8
295
.2
.4
.6
.8
10⁻⁵t

FIG. 2

FIG. 3

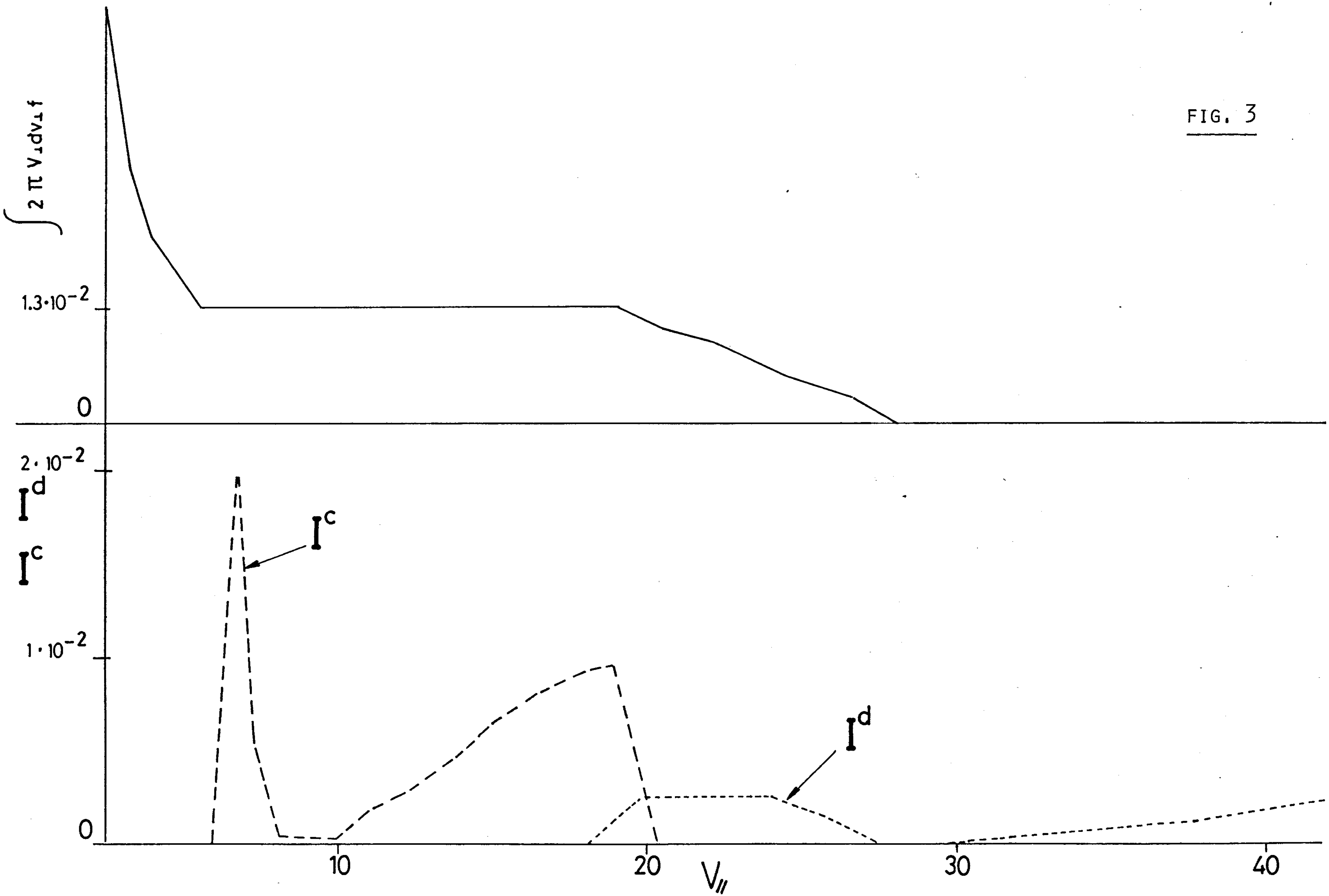

$\int 2\pi v_\perp dv_\perp f$
$1.3 \cdot 10^{-2}$
0
$2 \cdot 10^{-2}$
I^d
I^c
$1 \cdot 10^{-2}$
0
I^c
I^d
10
20
30
40
$V_{\parallel}$

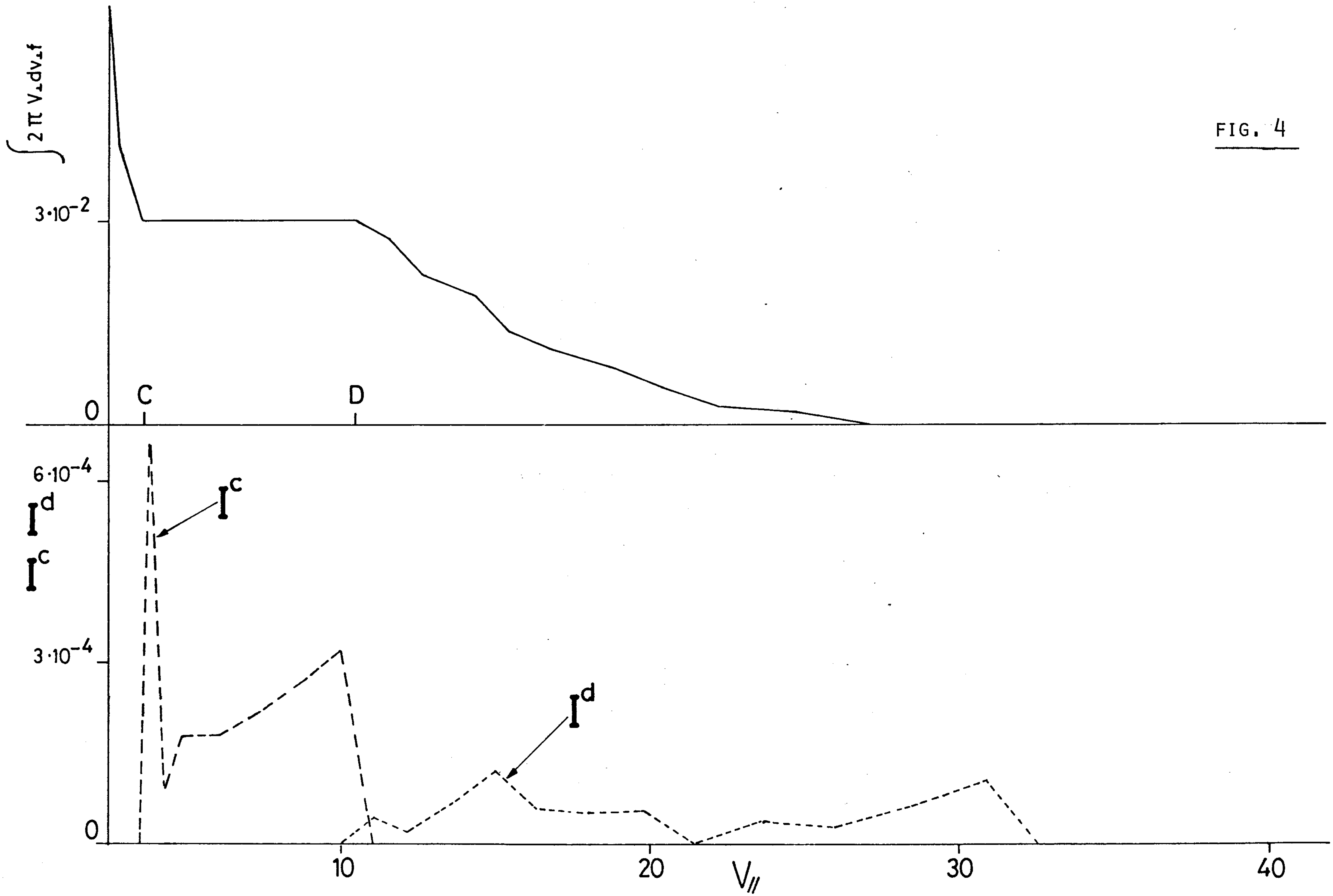

FIG. 4

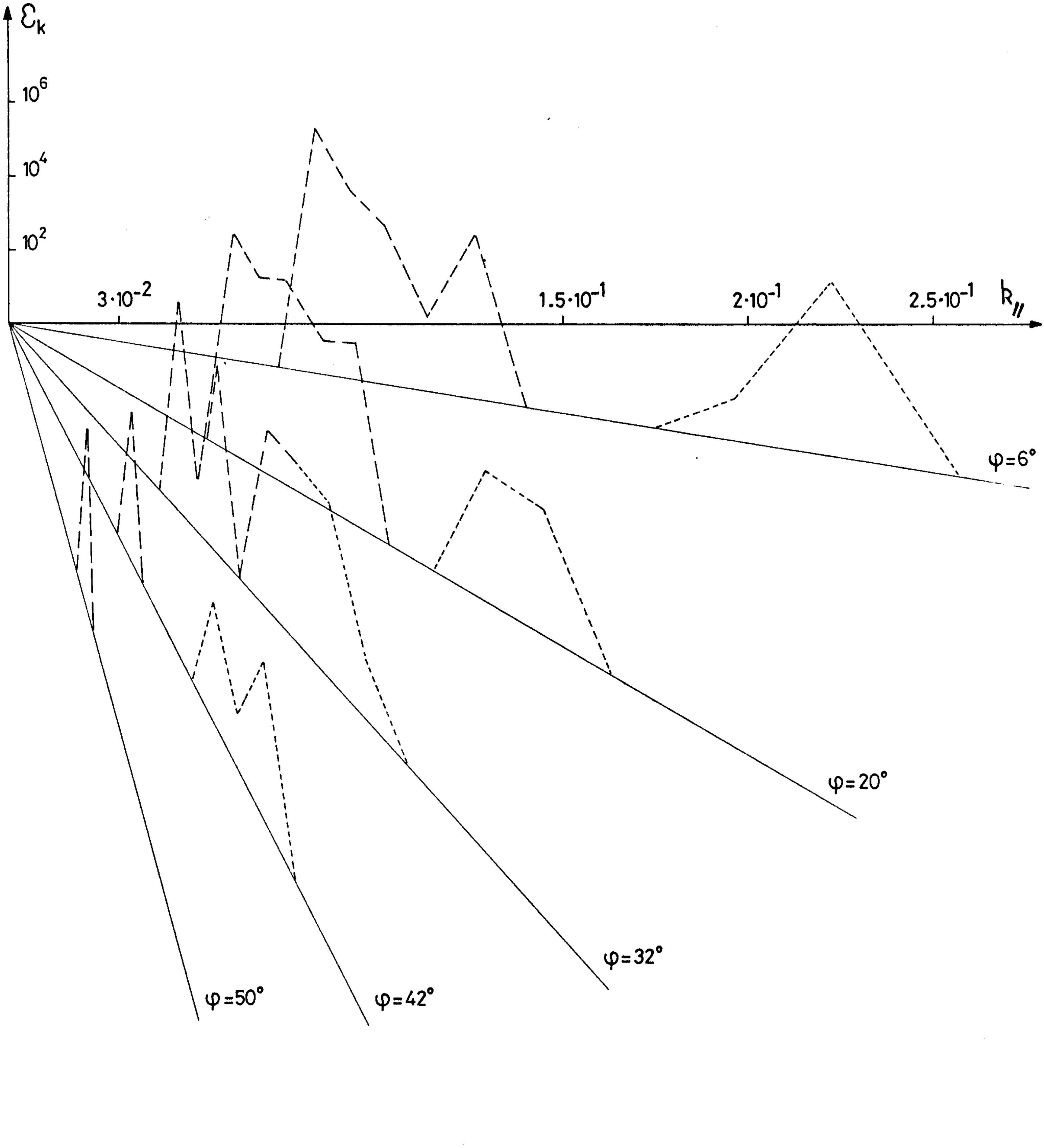

$\mathcal{E}_k$
10^6
10^4
10^2
$3\cdot10^{-2}$
$1.5\cdot10^{-1}$
$2\cdot10^{-1}$
$2.5\cdot10^{-1}$
$k_{//}$
$\varphi=6°$
$\varphi=20°$
$\varphi=32°$
$\varphi=42°$
$\varphi=50°$

FIG. 5